



ELSEVIER

Surface Science 472 (2001) 33–40

SURFACE SCIENCE

www.elsevier.nl/locate/susc

Substrate and morphology effects on photoemission from core-levels in gold clusters

Dan Dalacu, Jolanta E. Klemberg-Sapieha, Ludvik Martinu *

Groupe des Couches Minces (GCM), Department of Engineering Physics and Materials Engineering, École Polytechnique de Montréal, P.O. Box 6079, Station Centre-Ville, Montréal, Québec H3C 3A7, Canada

Received 8 August 2000; accepted for publication 16 October 2000

Abstract

The combination of X-ray photoelectron spectroscopy and spectrophotometry of supported gold clusters on SiO₂ reveals the importance of cluster morphology in determining core-electron binding energies. As-deposited films show a discontinuous dependence of the binding energy on gold content, associated with a transition from coagulated or partially coalesced clusters to isolated clusters. In contrast, annealed films exhibit a smooth increase in binding energy down to very low gold content. Comparison of the photoemission from annealed clusters deposited on and embedded in the insulating SiO₂, as well as clusters deposited on a conducting ITO substrate, was used to highlight the contributing factors that determine the core-electron binding energy and line-width, namely: (i) initial-state effects relating to the electronic structure, (ii) final-state effects relating to relaxation processes, and (iii) the cluster charge, including the influence of image charge screening. © 2001 Elsevier Science B.V. All rights reserved.

Keywords: X-ray photoelectron spectroscopy; Surface waves; Plasmons; Clusters; Gold

1. Introduction

The study of the electronic structure of small metal clusters has been indispensable in understanding the transition from the atomic to the solid state [1]. A good comprehension of the processes that occur in this transition region can help in the technological advancement of applications such as heterogeneous catalysis [2], nonlinear optics [3,4], and nanoscale electronics [5]. The preeminent technique for probing the electronic structure of small metal clusters, in particular, the evolution of the

valence-band and core-electron levels with cluster size, is photoelectron spectroscopy. This has resulted in numerous photoemission studies on supported metal clusters (see Mason [6] and references therein), which frequently use gold as a model material [7–16].

A significant effort has been devoted to the study of the core-level binding energies (CBE) and line-widths determined by X-ray photoelectron spectroscopy (XPS) in order to understand the changes in the initial-state electronic structure (valence-electron configuration) and final-state relaxation (extra-atomic response to the positively charged core hole created by photoionization) when going from bulk metal to atom (see, for example, DiCenzo and Wertheim [17]).

* Corresponding author. Tel.: +514-340-4099; fax: +514-340-3218.

E-mail address: lmartinu@mail.polymtl.ca (L. Martinu).

Changes in the valence-electron configuration and the associated valence-band narrowing as the size of the cluster decreases have been compared to the electron configuration changes that occur for surface atoms in bulk samples [18]. In the latter case, the valence-band narrowing is understood to arise from an s–d redistribution consisting of a reduction of the number of delocalized s states and d bulk states of bonding character and enhancement of the number of localized d states of non-bonding and anti-bonding character [19]. The resulting decrease of the energy between the center of the narrowed surface atom d-band and the Fermi level pulls the density of states to lower binding energy together with the core-levels. A CBE shift to lower energy is also expected with decreasing cluster size by virtue of the increasing number of surface atoms in the clusters.

Final-state relaxation processes in the bulk will decrease the CBE compared to that of an isolated atom [6]. This is expected from the decrease in conduction electron screening of the core hole produced by photoionization due to the discretization of the conduction band with decreasing particle size [20,21]. A further reduction will occur as the screening provided by the cores of neighbouring atoms decreases due to a reduction of the effective coordination (increase in the fraction of surface atoms which have a reduced coordination). The increase in the CBE with decreasing cluster size resulting from the disappearance of these bulk relaxation processes will be modulated by the substrate's ability to shield the final-state hole.

Competing with the above two fundamental processes is the possibility of cluster charging. Core-electron photoemission from a positively charged cluster (due to photoemission from a previous electron) will have a higher CBE as a result of the Coulomb attraction barrier, the increase in the CBE depending on the shape of the cluster [11] and image charge screening [22]. Whether or not charging comes into play depends on the ability of the substrate to neutralize the cluster within the lifetime of the core hole. This depends on the substrate density of states at the Fermi energy as well as the shape of the cluster (i.e. the contact area with the substrate).

Both initial- and final-state effects mentioned above will also influence the core-level line-width, characterized with the full width half maximum (FWHM) of the peak. In the case of the former effect, the line-width is expected to pass through a maximum at a surface to volume ratio (S/V) equal to one by virtue of the nonequivalence of the surface and volume atoms [12]. An increase in line-width is also expected with reduced screening, whether the reduction arises from a cluster size dependence of the conduction electron screening in the metal [23], or due to the surrounding environment (see Fuggle et al. [24] and references therein).

In this study, the CBE and line-width of gold clusters in the form of discontinuous films are investigated by XPS. The fundamental effects are distinguished from those produced by cluster charging through depositions on both insulating (SiO_2) and conducting (indium tin oxide, ITO) substrates as opposed to the more common amorphous carbon [6], which is only poorly conducting. We also compare the trends in binding energy and line-width with the optical properties of the films. Optical characterization of discontinuous films provides fruitful information concerning film microstructure (i.e. cluster size, shape, concentration ...) as a consequence of the excitation of surface plasmons, and concomitant absorption band in the visible [25]. The dependence of the surface plasmon resonance (SPR) on film microstructure is utilized to illustrate the distinctly different cluster morphologies that can occur in discontinuous films, which is important in understanding some of the observed trends in the XPS core-level energies and line-widths.

2. Experiment

The discontinuous gold films were deposited by radio-frequency (RF) magnetron sputtering from a 50 mm diameter gold target at 60 mTorr of Ar using an input RF power of 100 W for a self-bias of -350 V. To obtain films with different morphologies in a single deposition, the samples were displaced from the magnetron axis. This allowed us to control the volume fraction and size of the

particles comprising the films, both of which decrease with increasing distance from the magnetron axis [26]. In the present work, the samples are labeled A, B, . . . , H with the gold volume fraction and cluster size decreasing from A to H.

The films were deposited on glass substrates coated with ~ 20 nm of either SiO_2 or ITO. Additional samples were prepared for transmission electron microscopy (TEM) analysis on carbon-coated copper grids. One set of samples (including those for TEM) had an additional SiO_2 layer deposited on top. The SiO_2 layers were prepared by plasma-enhanced chemical vapor deposition (PECVD) using $\text{SiH}_4/\text{N}_2\text{O}$ chemistry in a high frequency plasma system described elsewhere [27,28]. A commercial ITO-coated glass was used with a sheet resistance of $10 \Omega/\text{square}$. Both annealed and as-deposited samples were studied. The post-deposition anneal was performed at 250°C in air for 5 h.

XPS analysis was performed in a VG ESCA-LAB 3 Mark II instrument with a non-monochromated MgK_α source (1253.6 eV) and a 0.8 eV resolution as measured from the FWHM of the $4f_{7/2}$ line of a continuous gold film. Optical transmission spectra were taken at normal incidence on a Perkin–Elmer Lambda 19 dual-beam spectrophotometer. TEM was performed on the samples deposited on carbon-coated copper grids using a Philips CM30 microscope. Image analysis was done using ImageTool from the University of Texas.

3. Results and discussion

3.1. Optical characterization of supported clusters

The transmission spectra of as-deposited and annealed films on SiO_2 and annealed films on ITO are shown in Fig. 1 together with the respective substrates. In all the spectra the SPR band is clearly visible indicating that gold exists in the form of small particles. The increase in transmission from sample A to E is predominantly due to a reduced gold content in the film, and thus reduced interband absorption [29].

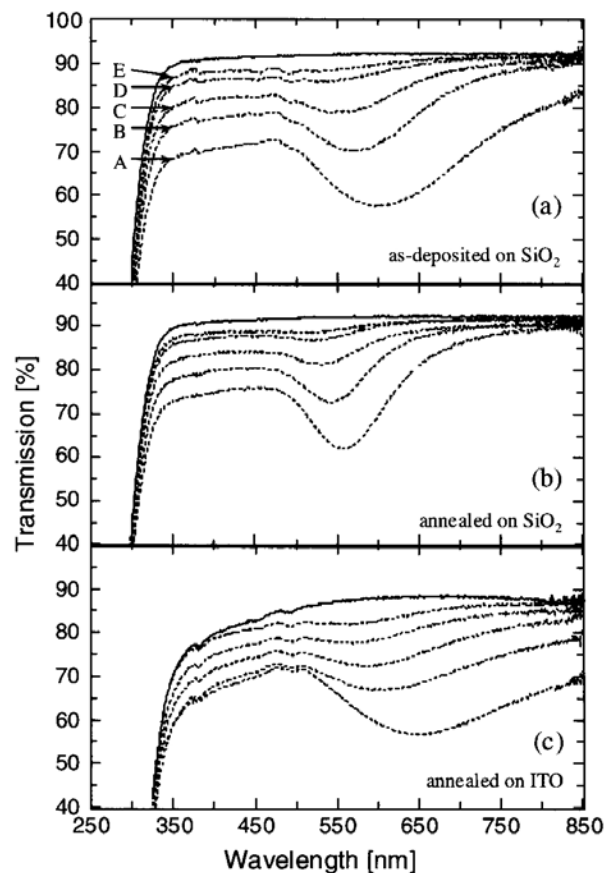


Fig. 1. Optical transmission spectra of discontinuous films deposited at varying distances from the magnetron axis: (a) as-deposited on SiO_2 , (b) annealed on SiO_2 , and (c) annealed on ITO. The labels A, B, . . . , E indicate decreasing gold content and cluster size. The solid lines correspond to the respective substrate spectra.

The blue-shift of the SPR with reduced gold content results from a decrease in dipole–dipole interactions [26,30]. A second contribution to the blue-shift arises from the presence of a core-polarization-free surface layer [31–33], the influence of which increases with decreasing particle size. The observed broadening of the SPR with decreasing gold content is also an effect of the finite size of the particles. In particular, the width is expected to increase linearly with inverse particle size [25], and is associated with the relaxation effects discussed in Section 1 [20,34].

The blue-shift and narrowing of the SPR upon annealing the samples on SiO_2 is indicative of a

transition from flattened particles, perhaps coagulated or partially coalesced, to that of larger, well-isolated spherical particles with a narrower size distribution [25,26,35]. Similar changes were observed when annealing the ITO samples. The red-shifted and broadened SPR bands for the clusters on ITO compared to the samples on SiO_2 are not due to morphology effects. They result, rather, from the higher refractive index of the ITO compared to SiO_2 which affects the shape of the SPR through its influence on the image charge interaction [26,36]. A second contribution is the possibility of charge transfer reactions at the Au/ITO interface, so-called chemical interface damping, CID [37]. CID effects have been used to account for the large broadening of the SPR for Ag in different reactive matrices [38], and is especially pronounced in Ag/ITO cermets [39].

3.2. X-ray photoelectron spectroscopy characterization of supported clusters

The Au 4f core-level spectra for the annealed samples on SiO_2 are shown in Fig. 2. Since the samples have been exposed to air, some degree of contamination is expected [40]. However, the 4f core-level spectra were well described using only two peaks corresponding to gold, as opposed to the multiple peaks required for gold present in its several characteristic oxidation states [41]. As such, we are confident that the peaks correspond to elemental gold.

The CBE shift and line-width of the Au 4f_{7/2} core-level peak with atomic concentration for the as-deposited and annealed samples on SiO_2 and annealed samples on ITO are shown in Fig. 3. The atomic concentration was determined using peak area and peak height sensitivity factors corresponding to a homogeneous sample, and, as such, is qualitative, and indicates only the relative concentration of gold. The plotted shift is relative to the bulk binding energy (84.0 eV) and has been corrected for substrate charging using the adventitious hydrocarbon C 1s peak at 284.8 eV as reference.

The as-deposited samples on SiO_2 show both an increase in CBE and line-width but with a different dependence on concentration above and below 5

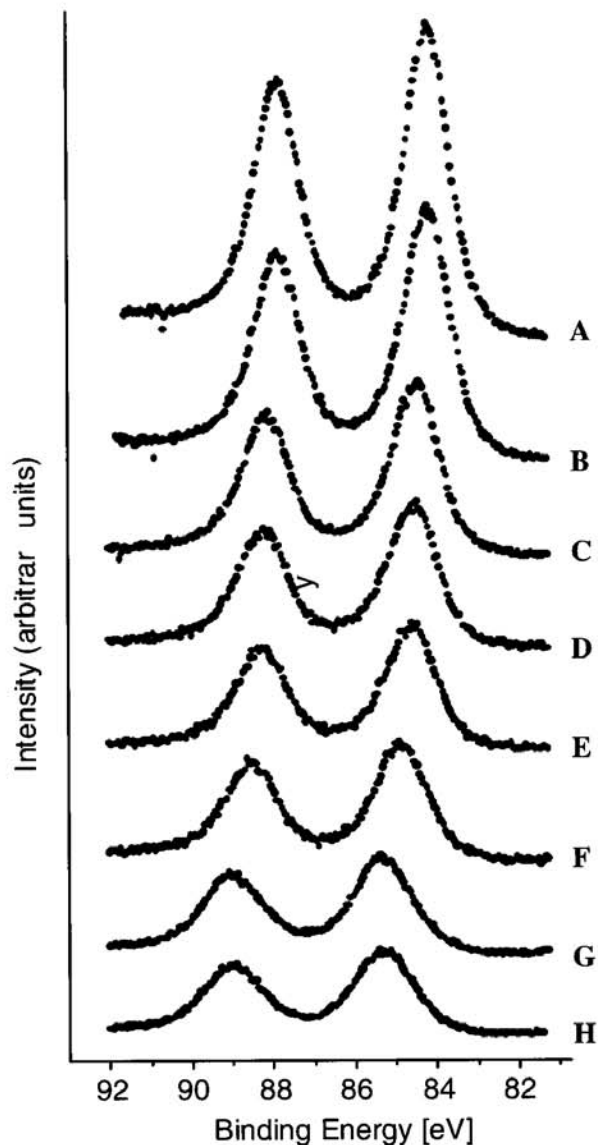


Fig. 2. The dependence of the Au 4f core-level spectra on atomic concentration for annealed films on SiO_2 . The labels A, B, ..., H indicate decreasing gold content and cluster size.

at.%. This concentration can be associated with a transition from a microstructure consisting of coagulated or partially coalesced flattened particles to that of a film consisting of isolated, more spherical clusters. We note that the CBE and line-width of the as-deposited films were sensitive to the X-ray flux. At higher flux, the CBE and line-width obtained corresponded to those of the annealed samples. We attribute this to local heating

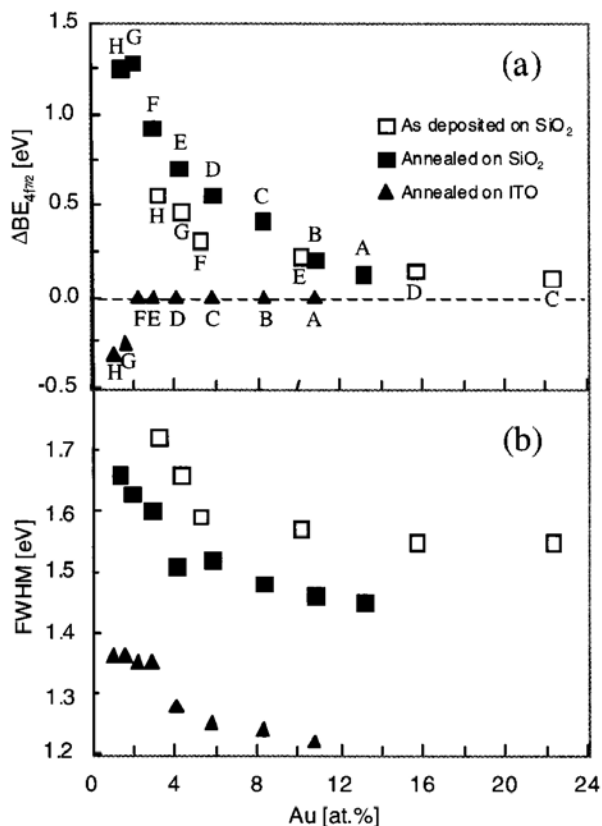


Fig. 3. The dependence of the CBE and line-width of the Au 4f_{7/2} peak on atomic concentration.

due to the irradiation which effectively anneals the samples. In fact, discoloration of the analysed spot, indicative of a change in microstructure, was clearly observed for the films with higher gold content.

The changes that occur upon annealing can be understood from the morphological changes suggested by the transmission spectra. The measured gold content is reduced as a result of decreased surface coverage as the clusters become more spherical. This also results in larger CBE shifts due to the decreased contact area of the clusters with the substrate (and, thus, less efficient charge neutralization). The accompanying decrease in cluster size distribution results in reduced line-widths. The smooth increase in the binding energy and line-width suggest that, unlike the as-deposited samples, the clusters here are well isolated, even at higher gold volume fractions. However, the sam-

ples on SiO₂ make evident a second transition at 2 at.% consisting of a negative CBE shift with decreasing concentration.

The transition at 2 at.% is more distinct for the annealed films on ITO since, in this case, the positive CBE shift due to cluster charging is absent: the reservoir of electrons in the ITO is able to neutralize the clusters within the lifetime of the core hole. (We note that charge transfer was already suggested by the severely broadened SPR of these films.) The highly polarizable conduction electrons in the ITO will also mask any change in the final-state relaxation of the particles by providing efficient screening of the core hole. The CBE shift and line-width for the ITO samples is, thus, due to initial-state electronic structure effects, and the second transition marks a S/V at which the surface atoms begin to play an important role in determining the CBE. We note that the CBE shift of surface atoms in bulk gold is -0.4 eV [18], compared to our value of -0.32 eV at 1 at.%.

3.3. X-ray photoelectron spectroscopy characterization of embedded clusters

The embedded clusters were prepared by depositing an additional SiO₂ layer (<10 nm) on top of the annealed discontinuous films deposited on SiO₂. These SiO₂/Au/SiO₂ structures were simultaneously deposited on carbon-coated copper grids for TEM analysis. The multi-layer structure ensures identical sets of samples since they are both surrounded by SiO₂, which also serves to minimize the influence of the probing beams (i.e. both the X-rays in the XPS analysis and the electrons in the TEM analysis). The TEM micrographs for samples deposited at different distances from the magnetron axis are shown in Fig. 4. The particle radius, R , and size distribution obtained from a detailed image analysis of a 378,600 nm² area (i.e. 400–4000 particles) are shown in Fig. 5.

The CBE shift and line-width versus $1/R$ is shown in Fig. 6. The observed CBE shifts are comparable to those of the annealed clusters supported on SiO₂ (Fig. 3). Apparently the increase in the CBE expected from the absence of image charge screening in embedded clusters (i.e. this screening is expected to reduce the charging shift

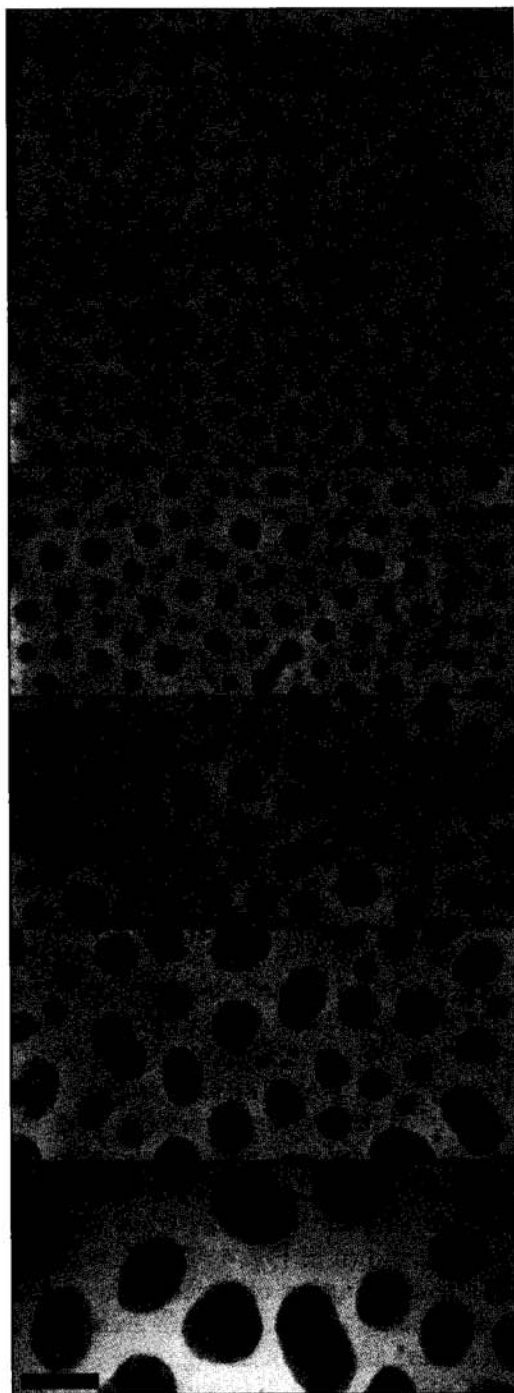


Fig. 4. TEM micrographs of films deposited at varying distances from the magnetron axis. Bar indicates 20 nm.

of supported clusters to about one-half compared to embedded clusters [22]) is compensated by an

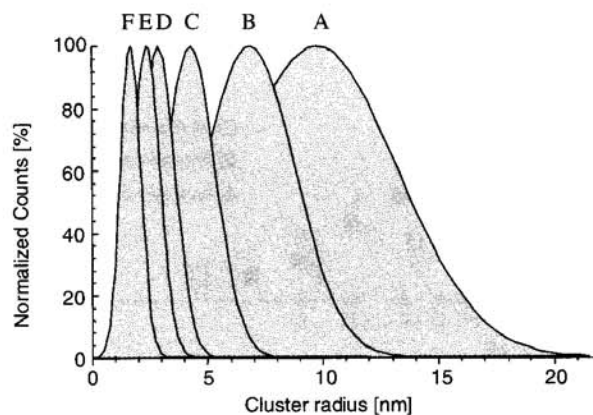


Fig. 5. Particle size distributions obtained from image analysis of the samples in Fig. 4.

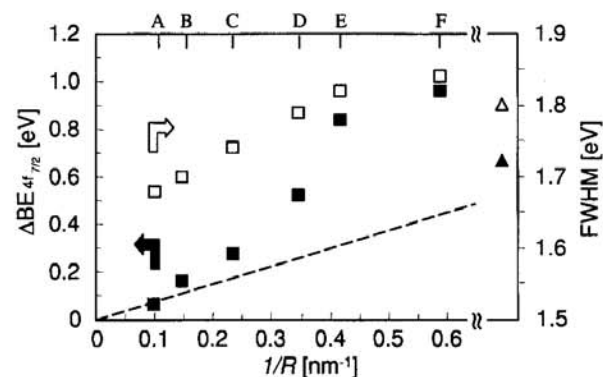


Fig. 6. The dependence of the CBE and line-width of the $\text{Au } 4f_{7/2}$ peak on reciprocal particle size for clusters in SiO_2 corresponding to TEM micrographs in Fig. 4. Triangles represent measurements on the 3-D film. Dashed line corresponds to the charging-induced shift: $\Delta\text{BE} \sim e^2/2R$.

increase in the polarization energy and perhaps a reduction in cluster charging due to the increased contact area with the SiO_2 . The CBE shift expected from the unit charge on a sphere ($e^2/2R$) is also shown in the figure, and does not account for the measured shift, suggesting that both relaxation effects and cluster charging have to be considered for the larger clusters. The observed increase in line-width compared to the supported clusters is surprising considering a decrease is that expected due to the increased screening provided by the surrounding SiO_2 [6].

The leveling-off of the increase in the CBE with decreasing cluster size is indicative of an increasing

contribution from initial-state effects (i.e. a decrease in the CBE with decreasing cluster size resulting from the increasing importance of the surface atoms) which moderates the relaxation-induced CBE shift. The initially linear dependence of the line-width on cluster size is a further indication of the influence of initial-state effects (i.e. $S/V \sim 1/R$), and the leveling-off at smaller clusters is suggestive of the peak anticipated for clusters with half the atoms on the surface and half in the volume, expected at $R \sim 1.2$ nm [42]. A contribution to the leveling-off of the line-width with decreasing cluster size is also expected from the decreasing size distribution observed in Fig. 5.

We have also attempted to prepare isolated gold atoms embedded in SiO_2 using simultaneous RF sputtering of the gold and PECVD of the SiO_2 [33], thereby limiting particle growth that arises from migration of gold atoms across the substrate surface. The 3-D films produced in this way have shown the same core-level [43,44] and valence band [45] behavior observed in the 2-D discontinuous films. A 230 nm thick film with a 7% gold volume fraction was deposited. The absence of gold particles consisting of more than a few atoms was verified from the transmission spectrum which showed no sign of the SPR (see Ref. [33], Fig. 3b).

Measurement of the CBE shift and line-width of the $4f_{7/2}$ level of the 3-D film gave 0.66 and 1.8 eV, respectively, both of which are smaller than the corresponding measurements on sample F in Fig. 4. The initial-state effect suggested by the measurements on the supported samples (i.e. decrease in CBE with decreasing gold content) is, thus, also observed to contribute to the CBE of the embedded clusters. Furthermore, the peak in the line-width versus $1/R$, expected from the distinct nature of the surface and volume atoms, is observed, and lies within the appropriate size range.

4. Summary and conclusions

We have demonstrated the influence of the microstructure of discontinuous gold films on XPS core-level energies and line-widths. Identically prepared samples give vastly different results depending on post-deposition heat treatments. The same

is true for the optical transmission spectra. We have applied the known dependence of the SPR absorption band on cluster morphology to draw the following conclusion: annealed films consist of well-isolated clusters with a small size distribution and can be characterized in terms of cluster radii. This allows reliable information concerning the fundamental processes (initial- and final-state effects) that influence the CBE and line-width to be determined. On the other hand, as-deposited films are likely to consist of coagulated and/or partially coalesced small clusters, the effects of which dominate over the fundamental processes.

XPS characterization of annealed discontinuous films deposited on both insulating and conducting substrates, as well as embedded in an insulating matrix, has allowed us to identify specific effects related to (i) electronic structure, (ii) relaxation, and (iii) cluster charge, including the influence of image charge screening.

Acknowledgements

The authors wish to acknowledge the expert technical assistance of Mr. G. Jalbert. This work was supported by the Natural Sciences and Engineering Research Council (NSERC) of Canada.

References

- [1] W.A. de Heer, Rev. Mod. Phys. 65 (1993) 611.
- [2] M. Valden, X. Lai, D.W. Goodman, Science 281 (1998) 1647.
- [3] D. Ricard, P. Roussignol, C. Flytzanis, Opt. Lett. 10 (1985) 511.
- [4] H.B. Liao, R.F. Xiao, J.S. Fu, H. Wang, K.S. Wong, G.K.L. Wong, Opt. Lett. 23 (1998) 388.
- [5] S.H.M. Persson, L. Olofsson, Appl. Phys. Lett. 74 (1999) 2546.
- [6] M.G. Mason, Phys. Rev. B 27 (1983) 748.
- [7] K. Liang, W. Salaneck, I. Aksay, Solid State Commun. 19 (1976) 329.
- [8] H. Roulet, G.D.J.M. Mariot, C.F. Hague, J. Phys. F 10 (1980) 1025.
- [9] S.T. Lee, G. Apai, M.G. Mason, Phys. Rev. B 23 (1981) 505.
- [10] L. Oberli, R. Monot, H.J. Mathieu, D. Landolt, J. Buffet, Surf. Sci. 106 (1981) 301.

- [11] G.K. Wertheim, S.B. DiCenzo, S.E. Youngquist, *Phys. Rev. Lett.* 51 (1983) 2310.
- [12] G.K. Wertheim, *Phase Trans.* 24–26 (1990) 203.
- [13] D.M. Cox, B. Kessler, P. Fayet, W. Eberhardt, Z. Fu, D. Sonderlicher, R. Sherwood, A. Kaldor, *Nanostructured Mat.* 1 (1992) 161.
- [14] K.J. Taylor, C.L. Pettiette-Hall, O. Cheshnovsky, T.E. Smalley, *J. Chem. Phys.* 96 (1992) 3319.
- [15] C.N.R. Rao, V. Vijayakrishnan, H.N. Aiyer, G.U. Kulkarni, G.N. Subbanna, *J. Phys. Chem.* 97 (1993) 11157.
- [16] T. Ogama, *J. Vac. Technol. A* 14 (1996) 1309.
- [17] S.B. DiCenzo, G.K. Wertheim, *Clusters Mol.* 1 (1990) 361.
- [18] P. Citrin, G.K. Wertheim, Y. Baer, *Phys. Rev. B* 27 (1983) 3160.
- [19] P.H. Citrin, G.K. Wertheim, *Phys. Rev. B* 27 (1983) 3176.
- [20] A. Kawabata, R. Kubo, *J. Phys. Soc. Jpn.* 21 (1966) 1765.
- [21] M.E. Lin, R.P. Andres, R. Reifenberger, *Phys. Rev. Lett.* 67 (1991) 477.
- [22] G.K. Wertheim, S.B. DiCenzo, *Phys. Rev. B* 37 (1988) 844.
- [23] P. Ascarelli, M. Cini, G. Missoni, N. Nistico, *J. Physique C2* 38 (1977) 125.
- [24] J.C. Fuggle, M. Campagna, Z. Zolnierok, R. Lässer, A. Platau, *Phys. Rev. Lett.* 45 (1980) 1597.
- [25] U. Kreibig, L. Genzel, *Surf. Sci.* 156 (1985) 678.
- [26] D. Dalacu, L. Martinu, *J. Opt. Soc. Am. B* 18 (2001), in press.
- [27] J.E. Klemberg-Sapieha, O.M. Kuttel, L. Martinu, M.R. Wertheimer, *Thin Solid Films* 93–94 (1990) 965.
- [28] L. Martinu, J.E. Klemberg-Sapieha, O.M. Kuttel, A. Raveh, M.R. Wertheimer, *J. Vac. Sci. Technol. A* 12 (1994) 1360.
- [29] M. Guerrisi, R. Rosei, P. Winsemius, *Phys. Rev. B* 12 (1975) 557.
- [30] T. Yamaguchi, M. Takiguchi, S. Fujioka, H. Takahashi, *Surf. Sci. Lett.* 138 (1984) 449.
- [31] A. Liebsch, *Phys. Rev. B* 48 (1993) 11317.
- [32] V.V. Kresin, *Phys. Rev. B* 51 (1995) 1844.
- [33] D. Dalacu, L. Martinu, *J. Appl. Phys.* 87 (2000) 228.
- [34] C. Yannouleas, R.A. Broglia, *Ann. Phys. (NY)* 217 (1992) 105.
- [35] D. Jarret, L. Ward, *J. Phys. D: Appl. Phys.* 9 (1976) 1515.
- [36] T. Yamaguchi, S. Yoshida, A. Kinbara, *Thin Solid Films* 18 (1973) 63.
- [37] H. Hovel, S. Fritz, A. Hilger, U. Kreibig, M. Vollmer, *Phys. Rev. B* 48 (1993) 18178.
- [38] B.N.J. Persson, *Surf. Sci.* 281 (1993) 153.
- [39] U. Kreibig, M. Gartz, A. Hilger, H. Hövel, in: M. Duncan (Ed.), *Advances in Metal and Semiconductor Clusters*, JAI, Greenwich, 1998, vol. 4, p. 345.
- [40] R.C. Baetzold, *J. Appl. Phys.* 47 (1976) 3799.
- [41] A. Domingue, L. Dignard-Bailey, E. Sacher, A. Yelon, T.H. Ellis, in: E. Sacher, J.-J. Pireaux, S.P. Kowalczyk (Eds.), *Metallization of Polymers*, vol. 440 ACS Symposium Series, American Chemical Society, Washington, DC, 1990, p. 272 (Chapter 20).
- [42] U. Kreibig, *Solid State Commun.* 28 (1978) 767.
- [43] L. Martinu, V. Pische, R. d'Agostino, *Metallization of Polymers*, vol. 440, in: E. Sacher, J.-J. Pireaux, S.P. Kowalczyk (Eds.), ACS Symposium Series, American Chemical Society, Washington, DC, 1990, p. 170 (Chapter 12).
- [44] D. Dalacu, A.P. Brown, J.E. Klemberg-Sapieha, L. Martinu, M.R. Wertheimer, S.I. Najafi, M.A. Andrews, in: W.W. Lee, R. d'Agostino, M.R. Wertheimer (Eds.), *Plasma Deposition and Treatment of Polymers*, MRS Symp. Proc., vol. 544, Materials Research Society, Warrendale, PA, 1999, p. 167.
- [45] R. Joerger, R. Gampp, A. Heinzl, W. Graf, M. Kohl, P. Gantenbein, P. Oelhafen, *Solar Energy Mat.* 54 (1998) 351.